Journal of Pharmaceutical Sciences 107 (2018) 654-661

Contents lists available at ScienceDirect

Journal of Pharmaceutical Sciences

journal homepage: www.jpharmsci.org

Pharmaceutics, Drug Delivery and Pharmaceutical Technology

Composite Alginate-Hyaluronan Sponges for the Delivery of Tranexamic Acid in Postextractive Alveolar Wounds

Ovidio Catanzano [1, 2, *], Vittoria D'Esposito [3], Pietro Formisano [3], Joshua S. Boateng [2], Fabiana Quaglia [1]

[1] Department of Pharmacy, University of Naples Federico II, Via D. Montesano 49, Naples 80131, Italy
[2] Department of Pharmaceutical, Chemical and Environmental Sciences, Faculty of Engineering and Science, University of Greenwich, Medway, Central Avenue, Chatham Maritime, Kent ME4 4TB, UK
[3] Department of Translational Medical Sciences, University of Naples Federico II, Via S. Pansini 5, Naples 80131, Italy

ARTICLE INFO

Article history:
Received 23 August 2017
Revised 15 September 2017
Accepted 22 September 2017
Available online 5 October 2017

Keywords:
alginate
biodegradable polymers
controlled delivery
wound healing
mechanical properties

ABSTRACT

The management of wounds in patients on anticoagulant therapy who require oral surgical procedures is problematic and often results in a nonsatisfactory healing process. Here, we report a method to prepare an advanced dressing able to avoid uncontrolled bleeding by occluding the postextractive alveolar wounds, and simultaneously, capable of a fast release of tranexamic acid (TA). Composite alginate/hyaluronan (ALG/HA) sponge dressings loaded with TA were prepared by a straightforward internal gelation method followed by a freeze-drying step. Both blank and drug-loaded sponges were soft, flexible, and elegant in appearance and nonbrittle in nature. Scanning electron microscopy analysis confirmed the porous nature of these dressings. The integration of HA influenced the microstructure, reducing the porosity, modifying the water uptake kinetic, and increasing the resistance to compression. TA release from ALG/HA sponges showed a controlled release up to 3 h, and it was faster in the presence of HA. Finally, an *in vitro* clotting test performed on human whole blood confirmed that the TA-loaded sponges significantly reduce the blood clotting index by 30% compared with ALG/HA_{20} sponges. These results suggest that, if placed in a socket cavity, these dressings could give a relevant help to the blood hemostasis after dental extractions, especially in patients with coagulation disorders.

Introduction

Tooth extractions, even if considered as minor oral surgery, are one of the most routinely performed treatments among dental surgical techniques, and like all surgical procedures often cause large socket wounds, particularly after large tooth extraction. Under normal conditions, the management of oral surgical wounds is simple, but for some category of patients, such as those on anticoagulant therapy, it is problematic and still controversial. Generally, when tooth extraction is required in such patients, the pharmacological therapy is reduced or stopped for several days before the surgery, increasing the risks of uncontrolled bleeding and, most of all, thromboembolism, which is considered a major complication.[1-3] However, a different approach based on the use of local hemostatic agents would make it possible to operate without any interruption or diminution of the anticoagulant treatment, avoiding risks caused by clogged blood flow due to suspending drug regimen.[4-6]

The term "socket healing" generally refers to a series of local alterations that arise in both hard and soft tissues to close the socket wound after tooth extraction and to restore tissue homeostasis.[7] The most common complication following tooth extractions is the alveolar osteitis (dry socket) which may develop when an inflammation of the alveolar bone occurs, resulting in intense pain and delayed wound healing.[8,9] Dry socket is often a consequence of the removal or dissolution of the blood clot at the site of the tooth extraction before the wound has healed.[10] During tooth extraction, the formation of a blood clot is essential because it serves as a protective layer over the underlying bone and nerve endings in the empty tooth socket. The clot also provides the foundation for the growth of new bone and for the development of soft tissue.

For this purpose, an advanced wound dressing able to control wound bleeding and enhance clot formation could be very useful for the prevention of alveolar osteitis and pain following tooth extraction. The wound dressing can act both as socket plug limiting

Conflicts of interest: The authors declare no conflicts of interests.
This article contains supplementary material available from the authors by request or via the Internet at https://doi.org/10.1016/j.xphs.2017.09.026.

* *Correspondence to:* Ovidio Catanzano (Telephone/Fax: +39 3479129889).
E-mail address: ovid@hotmail.it (O. Catanzano).

https://doi.org/10.1016/j.xphs.2017.09.026
0022-3549/

the bleeding, but also as a local release platform for different drugs, including antifibrinolytics. In particular, the association of tranexamic acid (TA) with postoperative compression showed good results in preventing postoperative bleeding.[6,11] TA was already widely used as mouthwash[12] or as socket irrigation immediately after extraction[13] to prevent postextraction bleeding in patients on warfarin. However, this approach exhibits several limitations such as poor handiness and control over the delivered dose, as well as poor efficiency due to bleeding, which tends to quickly wash out the drug away from the administration site.

Macroporous alginate (ALG) sponges are considered a very interesting platform system for local drug release, and for this purpose, they have been extensively developed for a wide range of applications, such as bone tissue engineering, wound dressing, and drug delivery.[14-16] Through the years, ALG has gained a leading role among the wound dressing materials due to peculiar characteristics including the high absorbency and the promotion of healing and epidermal regeneration.[15] Its natural origin and simple extraction process from marine brown algae biomass, associated with their characteristics in terms of biocompatibility and biodegradability under physiological conditions, make this polysaccharide ideal for use as socket-dressing materials.[17] Furthermore, it has been demonstrated that calcium alginate materials activate platelet and blood coagulation and for this reason, they have also been used as hemostatic dressings.[18]

Common techniques for producing macroporous ALG dressings from a hydrogel or a polymer solution include air drying,[19] solvent evaporation,[20] or freeze drying.[21] However, because of their hydrophilic polymeric backbones, ALG dressings easily dissolve in water unless radical, chemical, or physical crosslinks are present. To overcome this limitation, internal gelation of ALG through $CaCO_3$-GDL (d-glucono-δ-lactone) system has been recently proposed by our group as a versatile and straightforward strategy to obtain homogenous cross-linked composite ALG hydrogels.[22,23] In addition, we found that the integration of hyaluronan (HA), an extracellular glycosoaminoglycan extensively involved in all phases of wound healing[24] in these ionically cross-linked ALG matrix has proved to be a versatile strategy to promote the wound healing process. Beside its function as the main component of extracellular matrix and cartilage, HA is also an important component of both soft periodontal tissues such as gingiva and periodontal ligament and of the hard tissue, such as alveolar bone and cementum. For these reasons, as recently reported by Casale et al.,[25] the topical application of HA could have a positive action on the healing of mineralized and nonmineralized tissues of the periodontium. Moreover, a recent pilot study in dogs demonstrated how HA may enhance bone formation and accelerate wound healing in infected sockets.[26]

In this work, we present an alginate/hyaluronan (ALG/HA)–based composite sponge dressing loaded with TA useful for reducing bleeding after tooth extraction and, at the same time, reducing the risk of alveolar osteitis. Moldable, biocompatible, and bioresorbable dressing were prepared by internal gelation followed by a freeze drying to obtain solid macroporous sponges loaded with TA. The gradual release of calcium ions directly from the inside of an ALG solution results in a homogeneous crosslink, with consequent improved mechanical properties, and allow an easy integration and a uniform distribution of drugs that are soluble in hydrogels or aqueous solutions. We examined in depth the behavior of the sponges when they came in contact with simulated biological fluids, evaluating the swelling rates, the degradation behaviour, and the drug release in relation to the composition and to the microstructure of the sponges. The mechanical properties and the adhesion profile on a simulated wound surface were also evaluated. Finally, the *in vitro* toxicity of the platform was tested in normal adult human primary epidermal keratinocyte cell lines and hemostatic efficacy evaluated through an *in vitro* dynamic whole blood clotting test.

Materials and Methods

Materials

Sodium alginate (from *Macrocystis Pyrifera*, medium viscosity, 360 cps at 25°C) was purchased from Farmalabor (Italy). HA sodium salt from *Streptococcus equi* (1.5-1.8 × 10^6 Da), tranexamic acid (TA), GDL, calcium chloride dihydrate, potassium chloride, sodium chloride, sodium phosphate dibasic, calcium carbonate, and dimethylsulfoxide were obtained from Sigma–Aldrich (St. Louis, MO). Ethanol (laboratory grade) was purchased from Carlo Erba (Italy). Media, sera, and antibiotics for cell cultures were from ATCC (American Type Culture Collection). 3-(4,5-dimethylthiazol-2-yl)-2,5-diphenyltetrazolium bromide (MTT) was obtained from Fisher Scientific (Leicestershire, UK). Deionized ultrafiltered water was used throughout this study.

ALG/HA Sponge Preparation

A 2% w/v ALG solution containing 2 different HA amount (10% or 20% of ALG weight to give ALG/HA_{10} and ALG/HA_{20}, respectively) was prepared and gelled with a freshly prepared GDL solution as previously described.[22,27] To obtain TA-loaded ALG/HA sponges, TA was dissolved directly in the initial ALG/HA solution to give a final drug concentration of 2% (w/v). Solutions were cast in 24-well culture plate (1 mL) to form circular disks 5 mm in thickness and 15 mm in diameter. The well plates were capped, sealed with Parafilm®, and gelled on a horizontal surface at room temperature for 24 h. After gelation, the ALG disks were washed with deionized water, frozen overnight at −20°C, and then lyophilized at 0.01 atm and −60°C in a Modulyo apparatus (Edwards, Crawley, UK). The freeze-dried sponges were stored at room temperature under vacuum.

Physical Characterization

The bulk morphology of the ALG/HA sponge was analyzed through scanning electron microscopy (SEM). Samples were mounted on a metal stub by means of carbon adhesive tape and coated with a 20-nm thick gold/palladium layer with a modular high-vacuum coating system Emitech K575X. Images at different magnification were acquired using Quanta 200 FEG (FEI, Hillsboro, OR) microscope.

The average porosity of the ALG/HA sponge was determined by a fluid displacement method. Ethanol was chosen as the displacement liquid because it penetrates easily into the pores and did not induce shrinkage or swelling. The geometrical volume (V_s) of the sponge samples was calculated by measuring diameter and height, and the pore volume (V_p) was measured by ethanol displacement method. The dry sponges ($n = 3$) were weighed (W_0) and immersed in absolute ethanol at room temperature, and then placed in a degasser for 5 min to remove air bubbles from the sponge pores. After wiping gently with a filter paper to remove surface ethanol, samples were weighed immediately (W_e) to reduce ethanol evaporation. The porosity of the sponge was calculated according to Equation 1:

$$\text{Porosity} = \frac{V_p}{V_s} \times 100 = \frac{W_e - W_0}{\rho_e V_s} \times 100 \quad (1)$$

where ρ_e represents the density of ethanol (0.789 g/cm^3). An average value of 5 replicates for each sample was taken.

The density (ρ) of the sponge was calculated according to the Equation 2:

$$\rho = \frac{W_0}{V_s} \quad (2)$$

The pore mean diameters were calculated from the SEM images using the public domain *Image J software* (NIH, Bethesda, MD).

To measure the water retention rate, sponge samples ($n = 3$) were soaked in water for 30 min then carefully removed and placed in a centrifuge tube. The sponge was centrifuged at 3500 rpm for 3 min to eliminate the excess water, and the wet weight was recorded. Water retention rate (WR) was calculated according the Equation 3 below:

$$WR = \frac{M_h - M_d}{M_d} \times 100 \quad (3)$$

where M_h (g) is the weight of the sponge after centrifugation, and M_d (g) is the initial dry weight. An average value of 5 replicates for each sample was taken.

Thermogravimetric analysis was performed to estimate the amount of residual moisture in the lyophilized sponges. Samples ($n = 4$) weighing between 3 and 6 mg were placed in a previously weighted 70-μL aluminum crucible and a dynamic phase of heating at a rate of 10°C/min from ambient temperature to 200°C was applied under a constant stream of dry nitrogen using a Thermal Advantage 2950 thermogravimetric analysis system (TA Instruments, Crawley, UK). The percentage residual moisture was estimated from the weight loss using a TA Universal Analysis 2000 software.

Mechanical Properties and Degradation Behavior

To investigate the resistance to deformation of the freeze-dried sponges, a Texture Analyser (Stable Microsystems Ltd., Surrey, UK) equipped with 5 kg load cell and Texture Exponent-32® software program was employed. A 6-mm cylindrical stainless steel probe (P6 probe; Stable Microsystems Ltd.) was used in compression mode. The resistance to deformation ('hardness') was investigated by compressing 5 ALG or ALG/HA sponges at 3 different locations to a depth of 2 mm at a speed of 1 mm/s using a trigger force of 0.001 N to determine the effects of HA on the force-time profiles during deformation by compression.

The *in vitro* mucoadhesive properties of sponges were performed using the same apparatus but in tension mode. A 6.67% w/v gelatin solution was allowed to set as solid gel in a Petri dish (diameter 88 mm) and used to simulate a gingiva surface. The samples ($n = 5$) were attached to a 75-mm diameter probe using double-sided adhesive tape. 0.5 mL of phosphate buffer saline (PBS, NaCl 120 mM, KCl 2.7 mM, Na_2HPO_4 10 mM) at pH 7.4 supplemented with 2% (w/v) BSA were spread on gelatin to simulate a wet surface. The probe, lined with sponges, was set to approach the model wound surface with the following pre-set conditions: pre-test speed 0.5 mm/s; test speed 0.5 mm/s; post-test speed 1.0 mm/s; applied force 0.01 N; contact time 60.0 s; trigger type auto; trigger force 0.05 N; and return distance of 10.0 mm.[23] The stickiness to the wound surface was calculated from the maximum force required to detach the sponge from the model surface, and it is known as peak adhesive force (PAF). The total work of adhesion was represented by the area under the force versus distance curve, whereas cohesiveness was defined as the distance traveled by sponge till detached and calculated using the Texture Exponent-32® software.

Water Uptake

Water uptake was determined by placing the ALG/HA sponges in water. Three circular samples of 15 mm diameter were obtained from a 24-well culture plate. The initial weight of each sample was accurately recorded using an analytical balance, and then they were placed in 5 mL of water in a thermostatic bath at 37°C. Samples were taken out, excess water was carefully removed using tissue paper, and after being weighed were re-immersed in water. The sample weight was recorded at intervals of 1 h up to 6 h and then every 24 h from there onward until equilibrium was established. Water was replaced after every weight measurement. The percentage swelling ratio (*SR* %) at each time point was calculated using Equation 4:

$$SR\% = \frac{W - W_0}{W_0} \times 100 \quad (4)$$

where W is the mass of the swollen sample and W_0 is the mass of the initial dry sample. The equilibrium water content (EWC) percent was calculated by Equation 5:

$$EWC\ (\%) = \frac{W_e - W_d}{W_e} \times 100 \quad (5)$$

where W_e is the mass of the swollen sample at equilibrium and W_d is the mass of the dry sample at equilibrium.

In Vitro *Drug Release*

The *in vitro* release profile of TA from ALG and ALG/HA sponge matrix was evaluated in PBS at pH 7.4. TA-loaded sponges were incubated in 10 mL of PBS and placed in a thermostatic bath at 37°C. At scheduled time intervals, the release medium was withdrawn and replaced with the same volume of fresh medium. The supernatant was analyzed for TA content by an indirect method using a UV-vis spectrophotometer after derivatization with fluorescamine according to the method described by El-Aroud et al.[28] Briefly, TA samples were diluted 1:2 by volume in a fluorescamine solution at 0.5% (w/v) in ethanol and incubated in the dark at room temperature for 1 h before analysis. The absorbance of TA samples was measured at 390 nm using a Shimadzu 1800 spectrophotometer (Shimadzu, Japan) fitted out with a 1 cm quartz cell (Hellma, Germany). The linearity of the response was verified over the concentration range 5–100 μg/mL ($r^2 \geq 0.999$).

Biocompatibility Studies

Cell viability studies were performed on normal adult human primary epidermal keratinocyte cells (ATCC PCS-200-011) cultured in a complete culture medium consisting of dermal cell basal medium (ATCC® PCS-200-030) plus one keratinocyte growth kit (ATCC® PCS-200-040). The keratinocyte growth kit contains the following growth supplements: bovine pituitary extract, rhTGFα, L-glutamine, hydrocortisone hemisuccinate, insulin, epinephrine, and apotransferrin. Furthermore, the medium was supplemented with 10 IU/mL of penicillin and 10 μg/mL of streptomycin. Cultures were maintained in humidified atmosphere of 95% air and 5% CO_2 at 37°C. An indirect cytotoxicity assay was performed in accord with the international standard ISO 10993-5[29] using the MTT (3-(4,5-dimethylthiazol-2-yl)-2,5-diphenyltetrazolium bromide) tetrazolium reduction assay (details in Supplementary Information S1).

In Vitro *Dynamic Whole Blood Clotting Studies*

Human blood was collected from healthy volunteers ($n = 5$) and anticoagulated with acid citrate dextrose tube (20-mM citric acid, 110-mM sodium citrate, 5-mM D-glucose). The blood clotting test was performed as described by Ong et al.[30] Briefly, 300 μL of acid citrate dextrose (ACD)—whole blood was slowly dropped on the surface of a sponge dressing placed into a 50-mL polypropylene tube. Once the sponges were completely covered, blood coagulation was triggered adding to the samples 24 μL of 0.2-M $CaCl_2$ solution followed by 10 min of incubation in a thermostatic incubator at 37°C under gentle shaking. Red blood cells (RBCs) that are not trapped in the clot were hemolyzed with 25 mL of deionized water that was added by dripping water down the inside wall of the tubes without disturbing the clotted blood. The relative absorbance (A) of blood samples that had been diluted to 25 mL was been measured at 542 nm using a spectrophotometer (Infinite 200, Tecan). The absorbance of 300-μL ACD—whole blood in 25-mL deionized water was assumed to be 100 as a reference value. The blood clotting index (BCI) of blank and drug-loaded ALG and ALG/HA_{20} sponges was calculated by the Equation 6.

$$\mathrm{BCI} = \frac{100 \times (\text{A of blood which had been in contact with sample})}{\text{A of ACD whole blood in water}} \quad (6)$$

The BCI is correlated to the number of RBCs entrapped into the cloth, so as the BCI index raises, blood clotting decreases.

Statistical Analyses

Statistical analyses were undertaken using GraphPad Prism®, version 6.00 (GraphPad Software, La Jolla, CA, www.graphpad.com). Data were compared using a Student *t* test and a one-way ANOVA with Bonferroni post-test (parametric methods).

Results and Discussion

Preparation and Characterization of ALG and ALG/HA Sponges

Freeze drying, which can prevent the destruction of the porous structure during the removal of water, was adopted in the preparation of crosslinked sponges starting from hydrogels obtained by internal gelation (Fig. 1a). The freezing method is useful to obtain regular pore sizes since the sponge porosity is directly correlated with the size of the ice crystal formed during the freezing stage of the freeze-drying process.[21] In particular, Kang et al.[31] demonstrated how the sponges prepared at freezing temperatures near −20°C, develop a 3-dimensional structure with interconnected pores without the use of any additives and organic

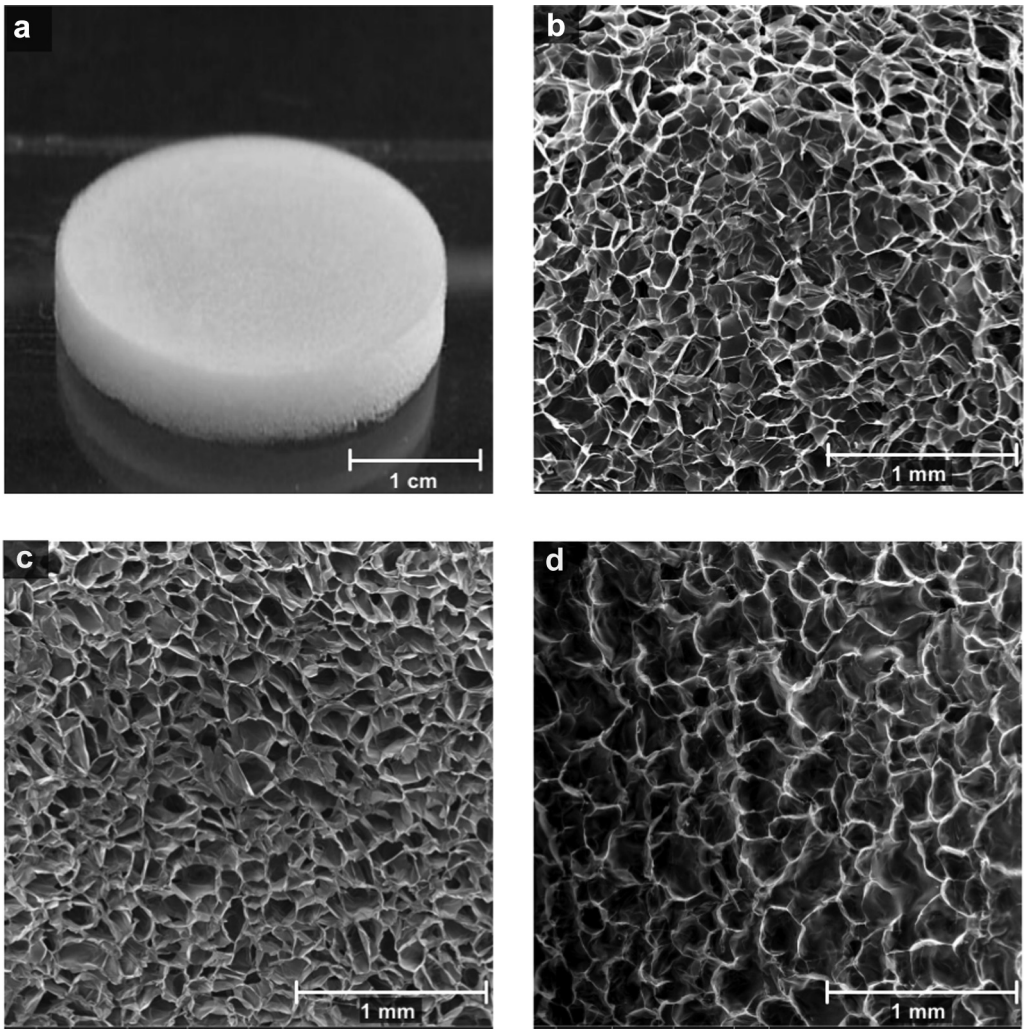

Figure 1. Image of an ALG/HA_{20} sponge after freeze drying (scale bar = 1 cm) (a). SEM images of ALG (b), ALG/HA_{10} (c), and ALG/HA_{20} (d) (scale bar = 1 mm).

Table 1
Characteristics of ALG Sponges

Characteristic	Porosity (%)	Pore Diameters (μm)	Density (mg/cm^3)	Water Absorption (%)	EWC (%)	Water Retention (%)	Residual Moisture (%)
ALG	56.61 ± 1.03	300 ± 70	30.76 ± 1.00	5103.95 ± 39.66	98.14 ± 0.02	75.4 ± 1.0	7.35 ± 0.03
ALG/HA$_{10}$	52.27 ± 3.21*	310 ± 14	34.74 ± 1.05*	4851.34 ± 63.77	98.08 ± 0.09	78.8 ± 4.1	7.38 ± 0.39
ALG/HA$_{20}$	47.70 ± 3.11*	320 ± 25	34.59 ± 1.85*	5070.04 ± 114.86	98.09 ± 0.07	77.1 ± 2.4	7.82 ± 0.31

*p <0.01 versus ALG.

solvents. The ALG/HA sponges were imaged by SEM. The surface of ALG sponge exhibited a random highly porous structure with interconnected pores with a size in the range of 300-500 μm. This highly porous structure is of utmost importance to ensure water absorption and mechanical strength, especially if an application as socket dressing is envisaged. However, it is worth to notice that from SEM images the microstructure of the ALG sponge (Fig. 1b) appears slightly different from the one of the ALG/HA sponges (Figs. 1c and 1d). In particular, the micrographs of the sponge of ALG alone showed relatively thinner walls with a visible interconnecting pore networks below the surface, differently than the ALG/HA sponge.

Water absorption (WA) and WR are 2 very important properties for sponge materials, which are highly dependent on their inherent structure and morphology. Values of porosity (P), WA, and WR for the various ALG/HA sponges are summarized in Table 1.

The porosity, calculated with the fluid replacement method, was in agreement with the morphological characterization by SEM. In comparison with ALG/HA, the porosity in the ALG crosslinked sponges is significantly higher (p <0.01 ALG/HA vs. ALG) suggesting a microstructure with deeper and interconnected pores. No significant differences in porosity were found between ALG/HA$_{10}$ and ALG/HA$_{20}$. Similarly, the presence of HA make the sponge significantly denser (p <0.01 ALG/HA vs. ALG). In the ALG/HA sponges, HA partially fills the gaps between the ALG chains, and this could explain the difference in porosity despite the similar pore diameters. However, this difference in porosity does not have a significant effect on the final amount of water that this system can absorb, being the value of water absorption and EWC similar. By comparing WR values for ALG and ALG/HA sponges after centrifugation, we can see how the WR of ALG/HA sponges was similar to ALG sponge, despite the different composition and the high hydrophilic character of HA.[32] In this case, it is probably the uniform and solid porous structure of crosslinked sponges that "lock" the water molecules and prevent the easy runoff of water.

Mechanical Properties

A postextraction socket dressing should have specific mechanical properties to serve as a therapeutic device and, at the same time, as a mechanical obstruction to bleeding. Periodontal dressing materials should be of slow-setting to allow manipulation and to create a smooth surface causing no irritation, should be flexible enough to withstand distortion and displacement, should be adhesive and coherent without being bulky, and must have the dimensional stability to prevent salivary leakage and plaque accumulation.[33] However, to date, there are no exact and standardized reproducible techniques to evaluate these properties. For this kind of dressing, the resistance to deformation (hardness) is a valuable physical property that can affect the material clinical behavior both during the application and during its adaptation to the tissues. Figure 2a shows how HA influences the resistance to deformation of the ALG/HA composite sponges. The addition of HA resulted in an increase in the 'hardness' with increasing concentration of HA and hence decreased the flexibility of the sponges.

Another physical property evaluated in this study was the adhesive properties of the sponge dressings on a simulated wet gingival surface. A dressing with good adhesive properties is especially important not only for an easy placing and retention but also considering its role in the prevention of microbial penetration. The adhesion profile was evaluated through measurement of the PAF, the total work of adhesion, and the cohesiveness, 3 parameters directly influenced by the physicochemical properties of the sponges such as the pore size distribution and the consequent hydration capacity.[34] In particular, PAF was used as a measure of the *in vitro* wound adhesive performance (Fig. 2b). The ALG sponges had a lower PAF (0.34 ± 0.1 N) compared with the ALG/HA$_{20}$ (0.69 ± 0.06 N), with an increasing trend proportional to the presence of HA. The same increasing trend appears in work of adhesion and cohesiveness. In general, adhesion properties depend

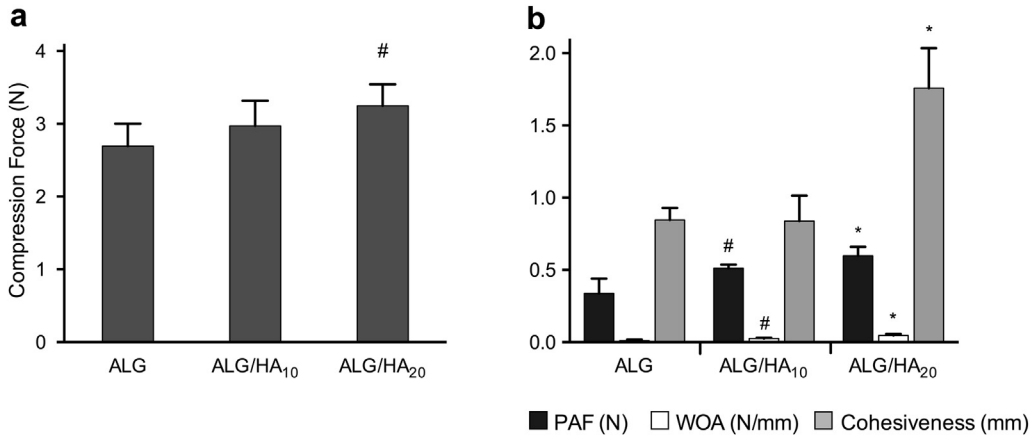

Figure 2. Resistance to deformation ('hardness') (a), and adhesion profiles (b) of ALG and ALG/HA sponges. Hardness was evaluated compressing the sponges at 3 different locations, checking the resistance to compression for the different formulations. The adhesion properties are represented by peak adhesive force (PAF), work of adhesion (WOA), and cohesiveness. Data are shown as means of 3 independent experiments with SD indicated by the error bar. *p <0.01, #p <0.05 versus ALG.

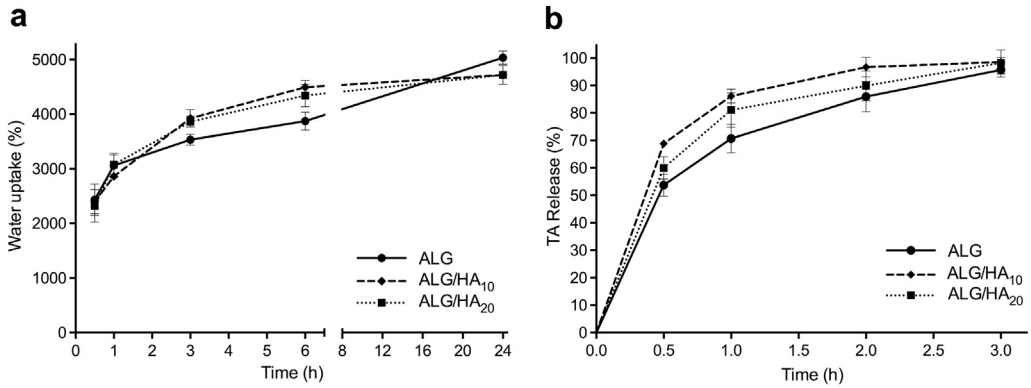

Figure 3. (a) Kinetics of water uptake of ALG and ALG/HA sponges. (b) TA release profile from ALG and ALG/HA sponges in PBS pH 7.4. Results are reported as mean ± SD ($n = 3$).

on the hydration capacity of the porous materials where a more rapid initial hydration and consequent more rapid entanglement between the polysaccharide chains and the wound surface which causes a higher dressing adhesion. In this case, the differences in all the 3 parameters considered could be attributed to the hydrophilic nature of HA which promotes the interaction between the sponges and the simulated wound environment probably due to the faster initial hydration.

Water Uptake and Drug Release From ALG/HA Sponge

The ability to absorb high amounts of fluids is essential to envisage a use of these systems as hemostatic dressings. Generally, for any advanced dressing, a high absorption capacity is considered to be beneficial in all the applications where great amounts of biological fluids were produced.[15] Moreover, a dressing capable of a rapid absorption of plasma may also directly contribute to the hemostasis by trapping the anticoagulant factors, which are normally present into the blood stream. Because the dressings can rapidly absorb plasma, the anticoagulant factors are separated from whole blood, resulting in a quick clotting of blood cells by activating the inherent clotting system.[35] In case of drug-loaded dressings, the drug release process is generally strictly related to the fluid absorption kinetic, which is in turn affected by sponge physical structure. For these reasons, the water absorption kinetics of ALG and ALG/HA sponges were carefully evaluated, and the results are shown in Figure 3a.

In contrast to EWC, the water absorption kinetics was influenced by the presence of HA in the sponge. The absorption curves of the ALG/HA hydrogels showed a higher rate of water uptake within the first 6 h of immersion (equilibrium swelling) as compared with ALG sponges, whereas after 24 h, all the formulations displayed similar water uptake. However, a difference in porosity does not seem to be the main determinant to explain water uptake kinetics. Nevertheless, the high hydrophilic and polyanionic character of HA[32] may lead to an increase of the hydrostatic pressure within the sponge and enhance its hydration rate.

The release of hydrophilic molecules from swellable sponges mainly depends on water uptake kinetics, thus pointing to the presence of HA as a key parameter in affecting the release rate. For application in bleeding wounds, a fast release of the hemostatic agent from the dressing is an essential property, and for this reason, the impact of matrix composition on drug release from loaded sponges was investigated. TA, a drug with well-known hemostatic properties, was loaded into the sponges and its release followed to evaluate the ability of the system to reduce bleeding on wound application. The ALG sponge showed the slowest release rate, whereas the presence of HA accelerated it (Fig. 3b). Comparison between the release profiles of TA and water uptake curves highlight that the water uptake reached over 70% of its final value in 3 h while in the same period almost 95% of TA is released. Thus, the swelling process peaks in 6 h, when all TA has been released. The incorporation of HA in the composite sponges significantly affected TA release profile because it causes a faster water absorption with a consequent larger burst effect. The faster water absorption also affects sponge's degradation *in vitro* (Supplementary Materials S2). The behavior of the sponges when in contact with a simulated biological fluid is correlated with the HA concentrations (Fig. S1), whose presence leads to a faster loss of the 3-dimensional structure. However, for ALG/HA sponges, this loss of structural integrity occurred after 7 days from the contact, giving an appropriate contact time for ensure the drug release and a mechanical contribution to hemostasis. On this basis, ALG/HA$_{20}$ providing the fastest TA release was selected for cell studies.

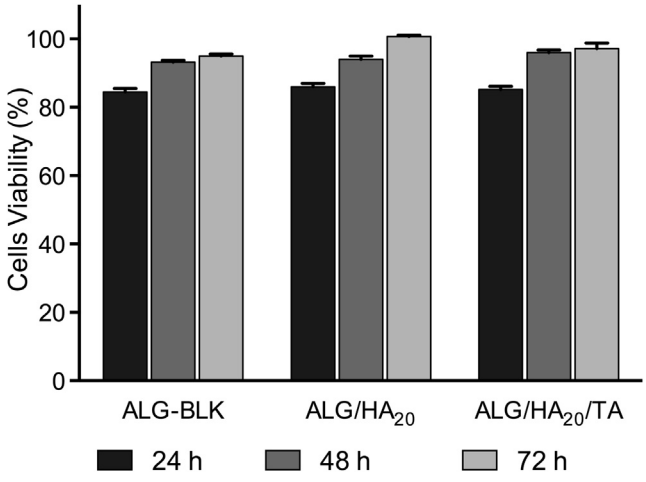

Figure 4. Effect of TA-loaded sponges on normal adult human primary epidermal keratinocyte cells viability. Cells (10,000 cells/well) have been seeded in 96-well culture plates in complete medium. The following day, the cells have been incubated with the extraction media for 24, 48, or 72 h in a humidified incubator. Cell viability has been determined, as optical density, by MTT. The results have been reported as percentage of viable cells compared with cells incubated in modified dermal cell basal medium in the absence of ALG sponges, considered as 100% viable cells. Bars represent the mean ± SD of triplicate determination in 3 independent experiments.

Biocompatibility Studies

Cytotoxicity test is a fast method to screen medical devices and provide predictive evidence of material biocompatibility. Biocompatibility of ALG and ALG/HA sponges loaded with TA was evaluated

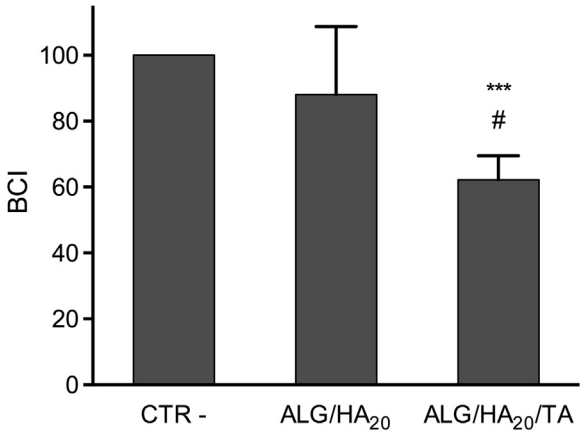

Figure 5. Effect of the ALG/HA_{20}/TA sponge on BCI, as measured by absorbance of hemoglobin from lysed uncoagulated RBCs. The BCI is correlated to the number of RBCs entrapped into the cloth, so as the BCI index raises as blood clotting decreases. $^{***}p$ <0.0001 versus CTR -, $^{\#}p$ <0.05 versus ALG/HA_{20}.

on normal human keratinocytes which play an important role in cell migration during normal wound healing. Figure 4 shows the effect of the sponges on the viability of keratinocyte cells assessed by indirect contact using a material extract previously conditioned with the samples to test. After indirect incubation of cells with the different sponges and the addition of the MTT dye, the formulations loaded with TA showed a toxicity profile not significantly different from the blank sponge, and the cell viability seems not to be influenced by the presence of HA and TA in the range of concentrations studied. All the formulation tested showed an initial cell mortality around 80%, a value that can be considered acceptable. In fact, the recommended guidelines for *in vitro* cytotoxicity for medical devices and delivery systems such as wound dressings (DIN EN ISO 10993-5) specifies that such materials can be deemed noncytotoxic for $\geq$70% cell viability after exposure.[29] Therefore, the results obtained in the present study show that all the formulated sponge could be considerate as biocompatible and generally safe.

Whole Blood Clotting Studies

The pro-coagulant properties of sponges loaded with TA were evaluated on ACD-human whole blood after 10 min of contact. After this time, the RBCs that were not trapped in the clot on the surface of dressing were hemolyzed and quantified using a spectrophotometer. In this case, higher absorbance values indicate a slower clotting rate. As shown in Figure 5, even when dispersed in ALG/HA sponges, TA was able to induce blood clotting. When human blood was incubated with TA-loaded sponges, the BCI was significantly reduced by 40% compared with negative control and by 30% compared with ALG/HA_{20} sponges. It has been already reported that HA can interfere with blood coagulation inhibiting platelet adhesion and aggregation and prolonging bleeding when administered systemically[36] or when used as a coating for biomedical devices.[37] However, in TA-loaded sponges, this anticoagulant activity related to HA was not evident. Taken together, these data demonstrate how using different concentration of HA, it was possible to modulate the mechanical and release characteristics of this composite sponge dressing preserving their pro-coagulant activity.

Conclusions

The aim of this study was the development of a biocompatible dressing able to fit the tridimensional postextractive alveolar cavity, ensuring a pharmacological and mechanical contribution to the hemostasis. ALG/HA sponges loaded with TA were prepared in a 2-step procedure starting from a crosslinked hydrogel with a freeze-drying method. ALG/HA sponges with various HA contents showed a porous morphology with an interconnecting network and a pore size related to the amount of HA in the formulation. Swelling studies and texture analysis also confirmed the effect of HA on porosity and on water uptake that results in an improved adhesive properties and a fast drug release. Once confirmed the biocompatibility, a blood clotting test was successfully performed confirming the capacity of these sponges to have a direct action on blood clotting.

Though further studies are needed to evaluate the *in vivo* blood clotting action of ALG/HA sponges, we can conclude that these dressings seem to be a very promising system for the management of uncontrolled bleeding in patients on anticoagulant therapy.

Acknowledgments

This research did not receive any specific grant from funding agencies in the public, commercial, or not-for-profit sectors. The authors are very grateful to Dr. Giulia Getti and Mr. Asif Ahmed for their help during biocompatibility studies.

References

1. Jeske AH, Suchko GD. Lack of a scientific basis for routine discontinuation of oral anticoagulation therapy before dental treatment. *J Am Dent Assoc*. 2003;134(11):1492-1497.
2. Kamien M. Remove the tooth, but don't stop the warfarin. *Aust Fam Physician*. 2006;35(4):233-235.
3. Madrid C, Sanz M. What influence do anticoagulants have on oral implant therapy? A systematic review. *Clin Oral Implants Res*. 2009;20(Suppl 4):96-106.
4. Blinder D, Manor Y, Martinowitz U, Taicher S. Dental extractions in patients maintained on oral anticoagulant therapy: comparison of INR value with occurrence of postoperative bleeding. *Int J Oral Maxillofac Surg*. 2001;30(6):518-521.
5. Evans IL, Sayers MS, Gibbons AJ, Price G, Snooks H, Sugar AW. Can warfarin be continued during dental extraction? Results of a randomized controlled trial. *Br J Oral Maxillofac Surg*. 2002;40(3):248-252.
6. Svensson R, Hallmer F, Englesson CS, Svensson PJ, Becktor JP. Treatment with local hemostatic agents and primary closure after tooth extraction in warfarin treated patients. *Swed Dent J*. 2013;37(2):71-77.
7. Araujo MG, Silva CO, Misawa M, Sukekava F. Alveolar socket healing: what can we learn? *Periodontol 2000*. 2015;68(1):122-134.
8. Cardoso CL, Rodrigues MT, Ferreira Junior O, Garlet GP, de Carvalho PS. Clinical concepts of dry socket. *J Oral Maxillofac Surg*. 2010;68(8):1922-1932.
9. Kolokythas A, Olech E, Miloro M. Alveolar osteitis: a comprehensive review of concepts and controversies. *Int J Dent*. 2010;2010:249073.
10. Birn H. Etiology and pathogenesis of fibrinolytic alveolitis ("dry socket"). *Int J Oral Surg*. 1973;2(5):211-263.
11. Bacci C, Maglione M, Favero L, et al. Management of dental extraction in patients undergoing anticoagulant treatment. Results from a large, multicentre, prospective, case-control study. *Thromb Haemost*. 2010;104(5):972-975.
12. Sindet-Pedersen S, Ramstrom G, Bernvil S, Blomback M. Hemostatic effect of tranexamic acid mouthwash in anticoagulant-treated patients undergoing oral surgery. *N Engl J Med*. 1989;320(13):840-843.
13. Carter G, Goss A. Tranexamic acid mouthwash—a prospective randomized study of a 2-day regimen vs 5-day regimen to prevent postoperative bleeding in anticoagulated patients requiring dental extractions. *Int J Oral Maxillofac Surg*. 2003;32(5):504-507.
14. Boateng J, Catanzano O. Advanced therapeutic dressings for effective wound healing-a review. *J Pharm Sci*. 2015;104(11):3653-3680.
15. Boateng JS, Matthews KH, Stevens HN, Eccleston GM. Wound healing dressings and drug delivery systems: a review. *J Pharm Sci*. 2008;97(8):2892-2923.
16. Valente JFA, Valente TAM, Alves P, Ferreira P, Silva A, Correia IJ. Alginate based scaffolds for bone tissue engineering. *Mater Sci Eng C*. 2012;32:2596-2603.
17. Laurienzo P. Marine polysaccharides in pharmaceutical applications: an overview. *Mar Drugs*. 2010;8(9):2435-2465.
18. Blair SD, Jarvis P, Salmon M, McCollum C. Clinical trial of calcium alginate haemostatic swabs. *Br J Surg*. 1990;77(5):568-570.
19. Andersen T, Melvik JE, Gaserod O, Alsberg E, Christensen BE. Ionically gelled alginate foams: physical properties controlled by type, amount and source of gelling ions. *Carbohydr Polym*. 2014;99:249-256.

20. Boateng JS, Auffret AD, Matthews KH, Humphrey MJ, Stevens HN, Eccleston GM. Characterisation of freeze-dried wafers and solvent evaporated films as potential drug delivery systems to mucosal surfaces. *Int J Pharm*. 2010;389(1-2):24-31.
21. Shapiro L, Cohen S. Novel alginate sponges for cell culture and transplantation. *Biomaterials*. 1997;18(8):583-590.
22. Catanzano O, D'Esposito V, Pulcrano G, et al. Ultrasmall silver nanoparticles loaded in alginate–hyaluronic acid hybrid hydrogels for treating infected wounds. *Int J Polymeric Mater Polymeric Biomater*. 2017;66(12):626-634.
23. Catanzano O, Docking R, Schofield P, Boateng J. Advanced multi-targeted composite biomaterial dressing for pain and infection control in chronic leg ulcers. *Carbohydr Polym*. 2017;172:40-48.
24. Frenkel JS. The role of hyaluronan in wound healing. *Int Wound J*. 2014;11(2):159-163.
25. Casale M, Moffa A, Vella P, et al. Hyaluronic acid: Perspectives in dentistry. A systematic review. *Int J Immunopathol Pharmacol*. 2016;29(4):572-582.
26. Kim JJ, Song HY, Ben Amara H, Kyung-Rim K, Koo KT. Hyaluronic acid Improves bone formation in extraction sockets with chronic pathology: a pilot study in dogs. *J Periodontol*. 2016;87(7):790-795.
27. Catanzano O, D'Esposito V, Acierno S, et al. Alginate-hyaluronan composite hydrogels accelerate wound healing process. *Carbohydr Polym*. 2015;131:407-414.
28. El-Aroud KA, Abushoffa AM, Abdellatef HE. Spectrophotometric and spectrofluorimetric methods for the determination of tranexamic acid in pharmaceutical formulation. *Chem Pharm Bull (Tokyo)*. 2007;55(3):364-367.
29. *ISO 10993-5 Biological Evaluation of Medical Devices, Part 5: Tests for Cytotoxicity, In Vitro Methods*. Geneva: International Standardization Organisation; 1992.
30. Ong SY, Wu J, Moochhala SM, Tan MH, Lu J. Development of a chitosan-based wound dressing with improved hemostatic and antimicrobial properties. *Biomaterials*. 2008;29(32):4323-4332.
31. Kang HW, Tabata Y, Ikada Y. Fabrication of porous gelatin scaffolds for tissue engineering. *Biomaterials*. 1999;20(14):1339-1344.
32. Toole BP. Hyaluronan: from extracellular glue to pericellular cue. *Nat Rev Cancer*. 2004;4(7):528-539.
33. Baghani Z, Kadkhodazadeh M. Periodontal dressing: a review article. *J Dent Res Dent Clin Dent Prospects*. 2013;7(4):183-191.
34. Pawar HV, Boateng JS, Ayensu I, Tetteh J. Multifunctional medicated lyophilised wafer dressing for effective chronic wound healing. *J Pharm Sci*. 2014;103(6):1720-1733.
35. Quan K, Li G, Luan D, Yuan Q, Tao L, Wang X. Black hemostatic sponge based on facile prepared cross-linked graphene. *Colloids Surf B Biointerfaces*. 2015;132:27-33.
36. Barbucci R, Lamponi S, Magnani A, et al. Influence of Sulfation on platelet aggregation and activation with Differentially Sulfated hyaluronic acids. *J Thromb Thrombolysis*. 1998;6(2):109-115.
37. Verheye S, Markou CP, Salame MY, et al. Reduced thrombus formation by hyaluronic acid coating of endovascular devices. *Arterioscler Thromb Vasc Biol*. 2000;20(4):1168-1172.